



## Enhancement in wind-driven sand transport by electric fields

Keld R. Rasmussen<sup>a</sup>, Jasper F. Kok<sup>b</sup>, Jonathan P. Merrison<sup>c,\*</sup>

<sup>a</sup> Department of Earth Sciences, University of Aarhus, Building 1520, Ny Munkegade, DK-8000 Aarhus C, Denmark

<sup>b</sup> Applied Physics Program, University of Michigan, Ann Arbor, MI 48109, USA

<sup>c</sup> Department of Physics and Astronomy, University of Aarhus, Building 1520, Ny Munkegade, DK-8000 Aarhus C, Denmark

### ARTICLE INFO

#### Article history:

Received 30 October 2008

Received in revised form

2 March 2009

Accepted 2 March 2009

Available online 9 March 2009

#### Keywords:

Interactions with particles and fields

Land/atmosphere interactions

Atmospheric electricity

Erosion and weathering

### ABSTRACT

Aeolian grain transport is a powerful erosion mechanism and a significant factor affecting atmospheric dynamics by the creation of particulate aerosols. Electric fields, both natural and man-made, occur widely at the Earth's surface in environments where granular material is found. Such electric fields may induce electrification of granular material and affect the transport dynamics of the grains. In this laboratory study we show that the influence of such electric fields is significant at field strengths well below that at which breakdown occurs and present a simple semi-empirical expression which allows this mechanism to be quantified.

© 2009 Elsevier Ltd. All rights reserved.

## 1. Introduction

In addition to the effects of erosion by aeolian (wind driven) grain transport, the suspension of large amounts (of order 1 billion tonnes per year) of mineral dust also constitutes a major climatic factor (Thomas et al., 2005; Tegen et al., 1996). Electric fields often occur at the earth's surface (both natural and man-made). Recent experimental laboratory studies have demonstrated and quantified the entrainment of grains from a surface using electric fields alone (Kok and Renno, 2006). The focus of this laboratory investigation, which utilizes an open circuit wind tunnel, is to quantify the effect of applied electric fields on the wind-induced transport of grains, such as sand and dust, especially close to threshold.

This research should also be seen in the context of growing interest in the role of electrification in sand/dust transport in desert areas (Shinbrot and Hermann, 2008; Kok and Renno, 2008; Schmidt et al., 1999; Zheng et al., 2006). Specifically in sand/dust-transporting environments electric fields in excess of 100 kV/m have been measured (Renno and Kok, 2008; Schmidt et al., 1998; Jackson and Farrell, 2006). This phenomenology is also being applied to other planets than earth, specifically Mars where aeolian dust activity is abundant (Merrison et al., 2004; Merrison et al., 2007).

### 1.1. Wind-driven grain transport

The transport of granular material by wind action occurs as air (gas) flowing over a surface induces velocity gradients and transfers stress to the surface. Here for an initially quiescent surface composed of uniform grains (i.e. size, mass and shape) as the stress ( $\tau$ ) above the surface exceeds a minimum value (the static threshold) the motion of grains from the surface occurs. Surface shear stress is difficult to measure directly, especially in an environment containing saltating sand grains. Therefore the friction velocity ( $u_*$ ) is introduced as  $\tau = \rho u_*^2$  where  $\rho$  is the mass density of the fluid. Though  $u_*$  has units of velocity the term is used to characterize the near-surface wind profile and it is generally accepted that for a horizontally homogeneous, thermally neutral boundary layer the friction speed (and hence the stress) is uniquely related to the vertical gradient of the horizontal velocity profile (White, 1991). Once active saltation has been initiated (i.e. when the friction velocity has exceeded the static threshold) momentum transfer from the wind flow to the sand bed may also occur through impacting grains. Here saltation can then be sustained at a substantially (around 16%) lower friction velocity, this is termed the dynamic threshold ( $u_{*d}$ ) (Bagnold, 1941). Even in laboratory studies the friction velocity can be difficult to establish reliably because precise velocity measurements must be made within the thin boundary layer immediately above the surface (Rasmussen et al., 1996). Experimentally an empirical relation for the saltation mass transport rate ( $q$ ) of sand has been seen to depend upon the product of the friction velocity and the surface shear stress (Bagnold, 1941) or more specifically on the friction velocity and the excess shear stress ( $\tau - \tau_t$ ) where  $\tau_t$

\* Corresponding author. Tel.: +45 89423723; fax: +45 86120740.

E-mail address: [merrison@phys.au.dk](mailto:merrison@phys.au.dk) (J.P. Merrison).

is the shear stress at the dynamic threshold of motion (Owen, 1964), i.e.  $q \propto u_* \times (\tau - \tau_t)$ .

Physically this relation may be understood by assuming that during steady-state saltation equilibrium is established such that grains are ejected from the surface at a sufficient rate that the surface shear stress is maintained at the threshold value. This occurs as the entrained sand grains modify the wind velocity gradient at the surface (by slowing down the wind). The vertical entrainment rate of sand grains is therefore linearly dependent upon the excess surface shear stress exerted by the fluid above the sand entrainment threshold. The wind-induced (horizontal) transport of entrained sand grains will be governed by the vertical entrainment rate (grain concentration) of the sand and the effective wind speed within the (near-surface) boundary layer. Hence the transport rate becomes a product of shear stress and friction velocity.

Improvement upon the simple Bagnold relation is the semi-empirical relation of Sørensen (1991);  $q = (\rho u_*^3/g) \times 0.4(1 - u_{*t}/u_*) \times (1 + k u_{*t}/u_*)$ , where  $g$  is the earth's gravitational acceleration ( $g = 9.81 \text{ m/s}^2$ ),  $k$  is an empirical parameter fitted to experimental data ( $k = 13.4$ ) and  $u_{*t}$  is the surface friction velocity at the dynamic threshold for grain saltation (for a specific sediment).

## 1.2. Electric fields

Electric fields at the earth's surface generally result from the combined electrification and separation of granular material while in suspension (Yair, 2008), an obvious example is in thunderstorms. One possible electrification process results from the impact of particulates of differing size and/or composition which transfers electrical charge; this is referred to as tribo-electrification or contact electrification. Electric fields are therefore often generated where strong winds and granular material are present, such as sand storms, dust storms/dust devils, snow storms (Renno and Kok, 2008; Schmidt et al., 1998; Jackson and Farrell, 2006). By definition thunderstorms create electric fields in excess of that required for electrical breakdown. In desert areas thunderstorms can be preceded by sand/dust storms and often do not result in precipitation (rain) reaching the ground (Pye and Tsoar, 1990). This is an example of an environment where electric field enhancement might be an important phenomenon i.e. at the edge of advancing dust storms and dust devils, where the wind speeds are above threshold and electric fields can be substantial (Jackson and Farrell, 2006).

If a sand bed was an ideal conducting layer the application of a (vertical) electric field would induce a lift stress ( $\tau_E$ ) given by  $\tau_E = \epsilon_0 E^2/2$ , where  $E$  is the electric field experienced by free electric charges above the surface and  $\epsilon_0$  is the permittivity of free space. At sufficiently large electric fields sand grains will have a larger electric force than the gravitational pull and may levitate. Such a phenomenon of electric-field-generated levitation has been observed in previous studies as well as being reproduced in this study (Kok and Renno, 2006).

In the case of a real sand bed consisting of multiple layers of grains the material will, however, resemble a poorly electrically conducting dielectric. Although leakage of electric charge through this layer allows electrification of the material (i.e. grains to become electrified) this may be a slow and non-uniform process.

Electrical charges within the dielectric sand layer experience a reduced electric-field-induced stress due to the electric field as given by:  $\tau_E = \epsilon_0 E^2/2k$ , where  $k$  is the dielectric constant of the sand (Kip, 1969). For dry sand  $k$  is expected to be in the range 2–4 (Kanagy and Mann, 1994). Note that if the charges lie above the dielectric surface this equation reverts to the case for charges in free space i.e.  $k = 1$ . Within the real sand bed the effective value of  $k$  is therefore expected to lie between 1 and 4 and has been obtained by fitting to the experimental data. In a similar way to the wind-driven sand transport model of Bagnold, which is employed here, this model of electrification treats the sand bed on a macroscopic scale rather than attempting to describe how individual sand grains behave (become electrified). It avoids the complexities of modeling the granular structure on a microscopic scale.

At wind speeds above the threshold for saltation another process for grain electrification, other than current leakage, can occur since impacting grains may allow (for example) contact electrification to occur at the sand bed surface.

## 2. Experimental simulation and procedure

In this section the wind tunnel design will be presented and the instrumentation used to quantify the wind flow and sand grain transport parameters. Relevant details of the experimental data acquisition will also be discussed.

### 2.1. Wind tunnel design

The structure of the wind tunnel used in this study is depicted in Fig. 1. The working section is 9 m long and has a rectangular

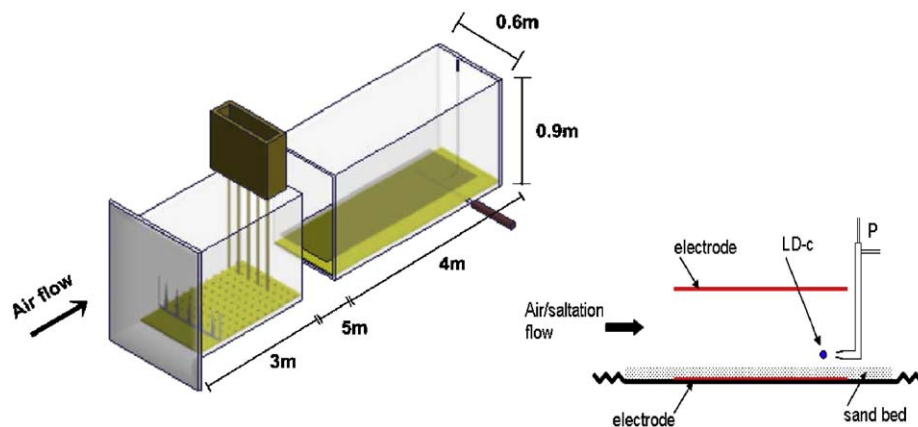


**Fig. 1.** The open-circuit wind tunnel is seen (left) showing the upwind air inlet with diffuser and bell mouth, followed by turbulence spires (for boundary layer modification), a roughness array and sand feed. In the downwind section the experimental working volume is seen with two electrodes placed above and below the sand bed, the laser doppler anemometer and Pitot-static wind sensor. A vertical section of this section is also shown (right), here the vertical positioning of the Pitot-static tube (P) and the laser-Doppler beam cross-over (LD-c) are indicated (10 mm above the sand bed).

cross section 0.60 m wide and 0.90 m high. The tunnel is constructed from wood with large glass panes inserted in the sides of the working section and in the roof. Free-stream wind speeds in the range 0–20 m/s can be generated. When the free flow at the wind tunnel entrance meets the sand bed the high surface wind speeds initially mobilize far more sediment than it can carry under steady-state conditions. This so called overshoot of saltation can be avoided with a combination of triangular turbulence spires and a 3 m array of cubic blocks (10 mm in dimension) placed at the wind tunnel entrance section (Shao and Raupach, 1992). This creates equilibrium between the upwind transition to the sand bed and the far downwind mobile sand bed (Irwin, 1981). The geometry of the spires and density of the roughness array were designed to be compatible with friction velocities in the range 0.2–0.3 m/s (Rasmussen and Iversen, 1993; Iversen and Rasmussen, 1999).

A uniform electric field was created in the region from 10 to 13 m downwind of the flow inlet by suspending a 250-mm-wide electrode at a height ( $h$ ) of 85 mm above the sand bed and a second electrode at a depth ( $d$ ) of 16 mm below the sand bed surface. The two electrodes were connected to the positive (upper) and negative/grounded terminals of a Brandenburg (60 kV) high-voltage generator, the voltage was monitored using a Brandenburg 139D HV meter.

The electrical resistivity of the sand was crudely measured by applying two metal electrodes across a sand layer and measuring the electrical resistance using a Giga-ohm meter (Norma, Unilap 150). Measurement uncertainties were large (depending on the humidity and contact force); however, a value of around  $10^{10}$ – $10^{11}$   $\Omega\text{m}$  was obtained. This corresponds to an average electrical charging time constant at the sand bed surface of around 0.1–1 s (Kanagy and Mann, 1994).

The electric field strength,  $E$ , above the sand (including the effect of the dielectric sand bed) is given by;  $E = V/(h+d/k)$  where  $V$  is the applied voltage. The dry sand was expected to have an (effective) dielectric constant of 1–4 as outlined in Section 1.2 (Kanagy and Mann, 1994); however, this value was adjusted to achieve agreement with the experimental data, this yielded a value of  $k = 2.6$ .

The uniform layer of sand grains was composed predominantly of quartz grains which had a diameter of around 254  $\mu\text{m}$  (212–300  $\mu\text{m}$ ). The mass density of the loose sand was measured to be  $1366 \pm 8$   $\text{kg/m}^3$ . The (bulk) mass density of individual grains was around 2650  $\text{kg/m}^3$ .

It is possible to 'seed' the sand transport (and impose the dynamic saltation threshold) by feeding grains into the roughness array. The rate could be adjusted depending on the aeolian granular transport rate in the wind tunnel.

## 2.2. Measurement Instrumentation

The surface friction velocity was quantified by performing wind speed measurements using a pitot-static tube connected to a differential pressure cell. The sensor was placed in the centre of the wind tunnel, around 150 mm before the downwind end of the electrodes and 10 mm above the sand bed such that the air speed could be monitored (Fig. 1).

The presence of the upper electrode in the wind flow unavoidably causes distortion of the surface boundary layer and values of threshold friction speed ( $u_{*t}$ ) derived from observations of the vertical velocity gradient below the suspended electrode are 15–40% below the canonical value for 242  $\mu\text{m}$  grains (Greeley and Iversen, 1985). Therefore estimates of the friction speed (above threshold) for a particular measurement period ( $u_*$ ) have been normalized to this expected value as given by  $u_* =$

$u_t/u_{10,t} \times u_{10}$ , where  $u_{10}$  is the measured (free-stream) flow speed obtained at 10 mm height above the sand bed,  $u_{10,t}$  is the corresponding flow speed measured at 10 mm height at the dynamic saltation threshold and  $u_{*t}$  is the expected surface friction velocity at threshold i.e. around  $u_{*t} = 0.2$  m/s (Iversen and Rasmussen, 1999). This is a crude correction method which, for instance, neglects variation of the aerodynamic roughness which will increase with saltation intensity (Raupach, 1991).

Uncertainty in the determination of  $u_*$  has been based on the experimental reproducibility obtained previously at different friction speeds (Rasmussen and Sorensen, 2008). Also good agreement is found in comparison with another method of quantifying wind flow using the fan rotation rate (Iversen and Rasmussen, 1999).

The saltation intensity was measured using a Dantec Flowlite laser Doppler anemometer (LDA) which is a single particle analysis technique relying on the creation of an interference pattern at the intersection of two coherent laser beams and the subsequent detection of scattered light. The sensor was placed outside the wind tunnel so as not to disturb the flow such that the measurement volume was positioned at the centre of the flow 10 mm above the sand bed and 200 mm before the downwind end of the upper electrode (see Fig. 1). In this way the number of moving grains at 10 mm height as well as their horizontal speed could be monitored for different air flows and different voltages across the electrodes. The LDA probe has a measurement cross section of around 0.2 mm  $\times$  4.2 mm. As a result of this relatively small cross section the sensor only records a small fraction of the total number of grains passing through the wind tunnel from which the total grain transport rate has been extrapolated. Therefore close to the saltation threshold, where the transport rate is low, measurement uncertainty is large as is the case when the measurement height is raised. The measurement height of 10 mm was chosen as a compromise between a desire to be within the main part of the saltation cloud, but high relative to the non-uniformity of the sand bed. Since ripples form rapidly due to saltation data acquisition times were made short (typically less than 200 s) before smoothing of the sand bed. For each friction speed alternate measurements were taken with and without an electric field.

Another experimental difficulty with this study is that during saltation, i.e. during data acquisition, evolution of the sand bed occurs. This can have the effect of changing (in this case usually raising) the effective measurement height of the LDA with respect to the sand bed surface. Similarly changes in the sand bed surface can alter the effective surface roughness and therefore the transport conditions. Also entrainment of electrified sand grains during saltation could modify the externally applied electric field especially at higher transport rates. These effects constitute systematic uncertainty in determining the mass transport and could account for the large (non-statistical) scatter in data points.

## 3. Experimental results and discussion

Two types of measurement series have been performed in this study. In one the grain transport has been quantified as the wind speed was varied both with and without application of an electric field. In the second measurement series the wind speed was constant and the electric field was varied. The results are presented in the following sections together with discussion.

### 3.1. The variation of the grain transport rate with wind friction speed

In Fig. 2 the average measured grain count rate is shown (measured at 10 mm height above the sand bed) for different

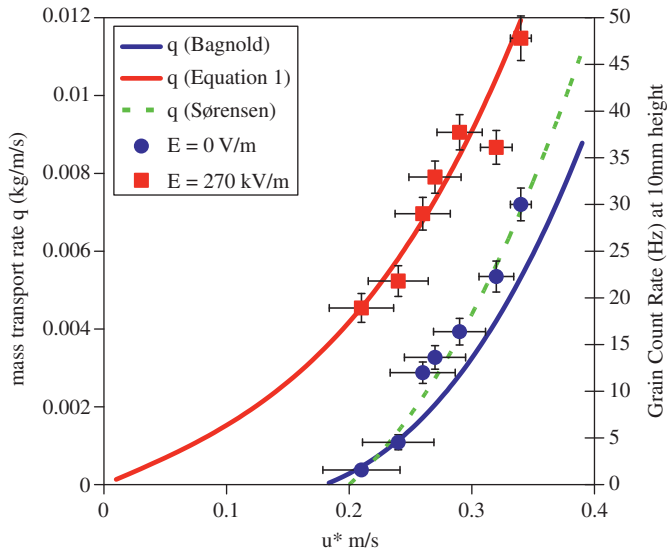


**Fig. 2.** Sand grain detection rate measured at 10mm above a sand bed as a function of friction speed for no electric field (●) as well as for a field of 270 kV/m (■). The dashed green line is the (zero electric field) mass transport theory of Sørensen, this has been used to normalize the grain count rate scale and the mass transport rate scale ( $q$ ). The solid blue line is the (zero electric field) mass transport theory of Bagnold. The solid red line is the semi-empirical theory proposed here (Eq. (1)) at an electric field of 270 kV/m. (For interpretation of the references to colour in this figure legend, the reader is referred to the web version of this article.)

near-threshold friction speeds both with and without application of an electric field, in this case 274 kV/m. Simple scaling of the axis has been performed in order to obtain the total mass transport rate such that the theory of Sørensen (1991) best fits the experimental data (without an electric field).

Normalization of the friction speed ( $u_*$ ) was performed by scaling to the predicted threshold value (around 0.2 m/s) based on the theory of Sørensen. For the theory of Bagnold the threshold friction speed was allowed to vary within experimental uncertainty and a value of 0.18 m/s gave an improved agreement (in the absence of an electric field).

A simple semi-empirical modification to the conventional transport rate expression has successfully reproduced the magnitude of this electric field effect and given generally good agreement with the experimental behavior, apparently adequately describing this phenomenon. This semi-empirical model has in principle no fitting parameters. Here, applying an electric field is assumed to induce electrical charge accumulation at the surface of the sand bed which applies a vertical stress ( $\tau_E$ ) due to the electric field.

As discussed in Section 1.2 the sand bed layer acts as a dielectric material modifying the applied electric field and transferred stress. The (vertical) stress of the electric field close to the surface of the dielectric sand bed will therefore have a dependence of the form:  $\tau_E = \varepsilon_0 E^2 / 2k$ , where  $k$  is the effective dielectric constant determined, by fitting, to have a value of 2.6.

Simplistically this electric-field-induced stress can modify the number (mass) of entrained sand grains in a way similar to the wind-induced surface shear stress, i.e. by modifying the shear stress in the rate equation of Bagnold. In other words the increased flux is as a result of the electric field helping to lift sand grains rather than considering the effect on the trajectories of individual grains. Based on this reasoning it is possible to derive an expression for the mass transport rate including the effect of the applied electric field.

$$q = \frac{Cu_*}{g} (\tau - \tau_t + \tau_E) \quad (1)$$

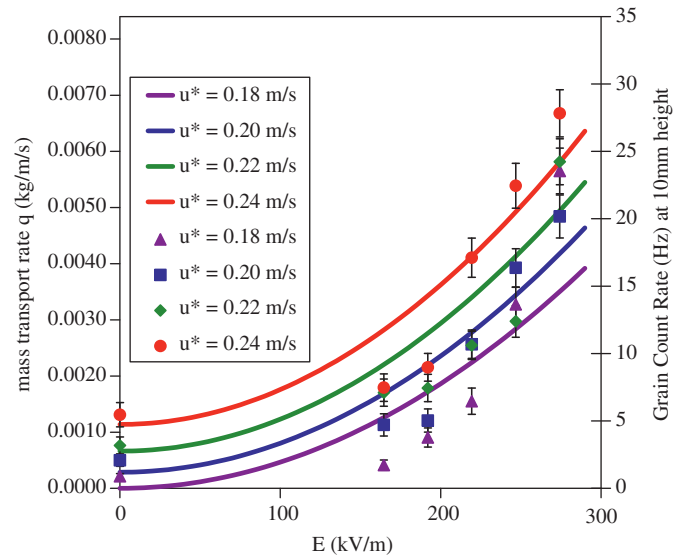


**Fig. 3.** Detected grain rate and (as in Fig. 2) mass transport rate determined at different friction speeds, at a height of 10mm above the sand bed, for increasing electric fields. The solid lines are the theory of Eq. (1) at the corresponding applied electric fields.

Here  $g$  is the gravitational acceleration and  $C$  is a dimensionless parameter dependent upon the grain size and morphology, in Bagnold's theory this has a value of 1.5 for uniform sand with grain size of 250  $\mu\text{m}$  (as in this study).

As can be seen the crude theory presented in Eq. (1) provides a reasonable (quantitative) reproduction of the enhancement in aeolian mass transport. This is despite the difficulty in this study, as in other experimental studies, to accurately quantify the mass transport rate and surface shear stress. Note that a similar modification could be applied to other rate equations than Bagnold's (for example Sørensen's) with similar, though not significantly improved agreement with this experimental data.

### 3.2. The variation of the grain transport rate with electric field strength

In this measurement series the wind speed was constant and the electric field was varied up to around 270 kV/m. These results are shown in Fig. 3 also for different near-threshold friction speeds. For comparison the onset of grain levitation was observed in the absence of wind at around 330 kV/m and according to Paschen's law electrical breakdown of air should occur in this electrode geometry at a field strength of around  $4 \times 10^6$  V/m (Paschen, 1889).

Examining these results it appears that although the general trend and approximate magnitude of the electric-field-enhanced grain saltation is reproduced the agreement at low electric fields (160–190 kV/m) is poor. Several factors, not easily incorporated into a simple model, may be responsible. One such factor involves the transfer of energy from the electric field to the saltation current which presumably occurs through the exchange of charge to the electrode(s) i.e. electrification of the grains close to the sand bed surface. If the time constant for this process is large compared to the removal of electrified grains by saltation then this may constitute a limiting factor and reduce the electric field enhancement. Electrification of sand grains could also occur by collisional processes which could complicate the dependence of grain transport on an applied electric field (Shinbrot et al., 2006).

Also in this study assumptions are made about the vertical distribution of saltating grains which may be affected by the

presence of an electric field and again introduce complexity to the process. These effects have not been addressed specifically in this study and it is hoped that this research stimulates further investigation of the phenomenon of electric field enhancement in aeolian processes, both on this and other planets. Emphasis should be placed on field work and modeling where the limitations of laboratory study can be eliminated.

#### 4. Conclusion

In this experimental investigation the aeolian transport rate of sand has been quantified under the influence of an applied (DC) electric field. This experiment for the first time quantifies the effect of electric fields on wind-driven granular transport and shows it to be highly significant at field strengths well below the atmospheric breakdown voltage and comparable to electric fields generated in nature. At electric fields in the range 160–280 kV/m increase in mass transport has been observed, in some cases in excess of an order of magnitude.

A simple semi-empirical expression has been successfully applied to the data. Here the sand bed has been treated as a dielectric film which under the influence of an electric field modifies the surface shear stress.

Although the electric fields generated in this study are significantly higher than those typically generated by man-made instrumentation, such as high-voltage transmission lines (10–50 kV/m), granular material with smaller grain size (than 240  $\mu\text{m}$ ) or with lower mass density could be (significantly) affected by this phenomenon at much lower electric field strengths. Examples might be dust silt/clay aggregates or snow. This may have particular relevance to Mars where dust aggregates appear to play a role in the ubiquitous aeolian transport of dust and where the low humidity may enhance electric field generation.

#### Acknowledgements

Thanks to Nilton Renno and Per Nørnberg for their support.

#### References

- Bagnold, R.A., 1941. *The Physics of Blown Sand and Desert Dunes*. Methuen, London.
- Greeley, R., Iversen, J.D., 1985. *Wind as a Geological Process on Earth, Mars and Venus*. (Cambridge Planetary Science Series). Cambridge University Press, Cambridge, pp. 78–79.
- Irwin, H.P.A.H., 1981. The design of spires for wind simulation. *Journal of Wind Engineering and Industrial Aerodynamics* 7, 361–366.
- Iversen, J.D., Rasmussen, K.R., 1999. The effect of wind speed and bed slope on sand transport. *Sedimentology* 46, 723–731.
- Jackson, T.L., Farrell, W.M., 2006. Electrostatic fields in dust devils: an analog to Mars. *IEEE Transactions on Geoscience and Remote Sensing* 44 (10), 2942–2949 (Part 2).
- Kanagy, S.P., Mann, C.J., 1994. Electrical properties of Eolian sand and silt. *Earth-Science Reviews* 36, 181–204.
- Kip, A.F., 1969. *Fundamentals of Electricity and Magnetism*, 2nd ed. McGraw-Hill Kogashuka, Tokyo, p. 146.
- Kok, J.F., Renno, N.O., 2006. Enhancement of the emission of mineral dust aerosols by electric forces. *Geophysical Research Letters* 33, L19S10.
- Kok, J.F., Renno, N.O., 2008. *Physical Review Letters* 100, 014501.
- Merrison, J., Jensen, J., Kinch, K., Mugford, R., Nørnberg, P., 2004. The electrical properties of Mars analogue dust. *Planetary and Space Science* 52, 279–290.
- Merrison, J.P., Gunnlaugsson, H.P., Nørnberg, P., Jensen, A.E., Rasmussen, K.R., 2007. Determination of the wind induced detachment threshold for granular material on mars using wind tunnel simulations. *Icarus* 191, 568–580.
- Owen, P.R., 1964. Saltation of uniform grains in air. *Journal of Fluid Mechanics* 20, 225–242.
- Paschen, F., 1889. Ueber die zum funkenübergang in luft, wasserstoff und kohlenäure bei verschiedenen drucken erforderliche potentialdifferenz. *Annalen Der Physik* 273 (5), 69–75.
- Pye, K., Tsoar, H., 1990. *Aeolian Sand and Sand Dunes*. Unwin Hyman, London, p. 15.
- Rasmussen, K.R., Iversen, J.D., 1993. A variable slope wind tunnel for testing wind-blown sand. In: *Proceedings of the Seventh US National Conference on Wind Engineering*. Vol. 2, University of California at Los Angeles, Los Angeles, pp. 643–552.
- Rasmussen, K.R., Iversen, J.D., Rautahemio, P., 1996. Saltation and wind-flow interaction in a variable slope wind tunnel. *Geomorphology* 17, 19–28.
- Rasmussen, K.R., Sorensen, M., 2008. Vertical variation of particle speed and flux density in aeolian saltation: measurement and modeling. *Journal of Geophysical Research—Earth Surface* 113 (F2), F02S12.
- Raupach, M.R., 1991. Saltation layers, vegetation canopies and roughness lengths. In: *Barndorff-Nielsen, O.E., Willetts, B.B. (Eds.), Acta Mechanica, Suppl. Vol. 1*, pp. 135–144.
- Renno, N.O., Kok, J.F., 2008. Electrical activity and dust lifting on Earth, Mars, and beyond. *Space Science Reviews* 137 (1–4), 419–434.
- Schmidt, D.S., Schmidt, R.A., Dent, J.D., 1998. *Journal of Geophysical Research* 103 (D8), 8997–9001.
- Schmidt, D.S., Schmidt, R.A., Dent, J.D., 1999. Electrostatic force in blowing snow. *Boundary-Layer Meteorology* 93 (1), 29–45.
- Shao, Y., Raupach, M.R., 1992. The overshoot and equilibrium of saltation. *Journal of Geophysical Research* 97 (D18), 20559–20564.
- Shinbrot, T., LaMarche, K., Glasser, B.J., 2006. Triboelectrification and razorbacks: geophysical patterns produced in dry grains. *Physical Review Letters* 96 (17) (Art. No. 178002).
- Shinbrot, T., Hermann, H.J., 2008. Static in motion. *Nature* 45, 773.
- Sørensen, M., 1991. An analytic model of wind-blown sand transport. In: *Barndorff-Nielsen, O.E., Willetts, B.B., (Eds.), Acta Mechanica (Suppl.)*. Vol. 1, pp. 67–81.
- Tegen, I., Lacis, A.A., Fung, I., 1996. The influence on climate forcing of mineral aerosols from disturbed soils. *Nature* 380, 419.
- Thomas, D.S.G., Knight, M., Wiggs, G.F.S., 2005. Remobilization of southern African desert dune systems by twenty-first century global warming. *Nature* 435, 1218.
- White, F.M., 1991. *Viscous Fluid Flow*. McGraw-Hill, New York, 611pp.
- Yair, Y., 2008. Charge generation and separation processes. *Space Science Reviews* 137, 119–131.
- Zheng, X.J., Huang, N., Zhou, Y., 2006. The effect of electrostatic force on the evolution of sand saltation cloud. *European Physical Journal E* 19 (2), 129–138.